Intermolecular Proton−Hydride Bonding in Ion Pairs: Synthesis and Structural Properties of $[K(Q)][MH_5(P^iPr_3)_2]$ (M = Os, Ru; Q = 18-crown-6, 1-aza-18-crown-6, 1,10-diaza-18-crown-6)

Kamaluddin Abdur-Rashid, Dmitry G. Gusev, Alan J. Lough, and Robert H. Morris*

Department of Chemistry, University of Toronto, 80 St. George Street, Toronto, Ontario M5S 3H6, Canada

Received November 2, 1999

The salts $[K(Q)][MH_5(P^iPr_3)_2]$ (**1Os**, **1Ru**, Q = 18-crown-6; **2Os**, **2Ru**, Q = 1-aza-18-crown-6; **3Os**, **3Ru**, Q = 1,10-diaza-18-crown-6) were prepared by the reaction of $OsH_2Cl_2(PiPr_3)_2$ or $RuCl_3$/2.5$PiPr_3$ with KH in the presence of one of these crown ethers under an atmosphere of H_2 and were characterized by NMR and infrared spectroscopy, elemental analysis, and single-crystal X-ray diffraction. The X-ray structures of **3Os** and **3Ru** indicate that short intermolecular proton−hydride interactions between the hydrides of the anion and the NH moieties of the cation cause the self-assembly of one-dimensional networks of pentagonal bipyramidal $[MH_5(P^iPr_3)_2]^-$ anions and $[K(diaza\text{-}18\text{-}crown\text{-}6)]^+$ cations. The X-ray structures of **2Os** and **2Ru** indicate that these also form one-dimensional chains due to MH···HN and weak MH···HC interactions between the hydrides of the anions and the NH and methylene CH of the $[K(aza\text{-}18\text{-}crown\text{-}6)]^+$ cation. The MH···HN distance is 1.7 Å for both **2Os** and **2Ru** and 1.9 and 1.8 Å for **3Os** and **3Ru**, respectively. These distances were calculated by assigning a value of 1.0 Å to the N−H bond length and using the refined average Os−H and Ru−H distances of 1.56(4) and 1.58(3) Å observed in **1Os** and **1Ru**. Values of 2.2 and 2.1 Å were similarly obtained for the MH···HC distances in **2Os** and **2Ru**, respectively, using a value of 1.09 Å for the C−H bond length. The solid-state infrared spectra of **2Os**, **3Os**, **2Ru**, and **3Ru** show shifts in the NH, OsH, and RuH bands to lower frequencies relative to the free NH bands in $[K(1\text{-}aza\text{-}18\text{-}crown\text{-}6)][BPh_4]$ and $[K(1,10\text{-}diaza\text{-}18\text{-}crown\text{-}6)][BPh_4]$ and unperturbed OsH and RuH bands in **1Os** and **1Ru**. Solution NMR and infrared spectra and T_1, NOE, and NOESY experiments demonstrate that the MH···HN interactions persist in solutions of these complexes. The THF solutions of the salts containing proton−hydride bonds undergo efficient H/D exchange with D_2 gas, resulting in deuteration of the hydrides of the $[MH_5(P^iPr_3)_2]^-$ anion and the NH hydrogens of the $[K(1,10\text{-}diaza\text{-}18\text{-}crown\text{-}6)]^+$ cation. On the other hand, complexes **1Os** and **1Ru** that do not have MH···HN bonding do not undergo H/D exchange with D_2 gas. The relative strength of the proton−hydride bonds in the osmium and ruthenium complexes, as evidenced by their NMR and infrared spectral characteristics, is related to the magnitude of the acid dissociation constants of the respective conjugate acids of the anions.

Introduction

The ubiquitous role of hydrogen bonding in determining the physical and chemical characteristics of materials and influencing various fundamental chemical functions such as molecular conformation, species recognition, and selectivity is well-known.[1−7] The hydrogen bonds involved are classical ones in which the proton acceptor is an electronegative element (F, N, O, S). Unconventional or nonclassical hydrogen bonding in which the proton acceptor is a hydride hydrogen is a more recently identified phenomenon[8−12] and has been demonstrated to be characteristic of transition metal hydrides[1,13−20] as well as hydrides of main group elements, particularly

(1) Yao, W. B.; Crabtree, R. H. *Inorg. Chem.* **1996**, *35*, 3007−3011.
(2) Whitesides, G. M.; Simanek, E. E.; Mathias, J. P.; Seto, C. T.; Chin, D. N.; Mammen, M.; Gordon, D. M. *Acc. Chem. Res.* **1995**, *28*, 37.
(3) Whitesides, G. M.; Mathias, J. P.; Seto, C. T. *Science* **1991**, 254.
(4) Lehn, J. M. *Angew. Chem., Int. Ed. Engl.* **1990**, *29*, 1304.
(5) Subramanian, S.; Zarowotko, M. J. *Coord. Chem. Rev.* **1994**, *137*, 357−401.
(6) Desiraju, G. R. *Acc. Chem. Res.* **1991**, *24*, 290−296.
(7) Chang, Y. L.; West, M. A.; Fowler, F. W.; Lauher, J. W. *J. Am. Chem. Soc.* **1993**, *115*, 5991.
(8) Stevens, R. C.; Bau, R.; Milstein, D.; Blum, O.; Koetzle, T. F. *J. Chem. Soc., Dalton Trans.* **1990**, 1429.
(9) Lee, J. C.; Peris, E.; Rheingold, A. L.; Crabtree, R. H. *J. Am. Chem. Soc.* **1994**, *116*, 11014−11019.
(10) Peris, E.; Lee, J. C.; Crabtree, R. H. *J. Chem. Soc., Chem. Commun.* **1994**, 2573.
(11) Lough, A. J.; Park, S.; Ramachandran, R.; Morris, R. H. *J. Am. Chem. Soc.* **1994**, *116*, 8356−8357.
(12) Park, S. H.; Ramachandran, R.; Lough, A. J.; Morris, R. H. *J. Chem. Soc., Chem. Commun.* **1994**, 2201−2202.
(13) Crabtree, R. H.; Eisenstein, O.; Sini, G.; Peris, E. *J. Organomet. Chem.* **1998**, *567*, 7−11.
(14) Crabtree, R. H. *J. Organomet. Chem.* **1998**, *557*, 111−115.

10.1021/om9908837 CCC: $19.00
Publication on Web 02/03/2000

boron.[21−26] This interaction is believed to be involved in intermediates or in the transition states of hydride protonation mechanisms to generate the η^2-H_2 ligand and the reverse reaction, η^2-H_2 deprotonation.[27] An attractive interaction is usually suggested when the H···H distance in the proton−hydride bond is less than 2.4 Å, a distance that represents twice the van der Waals radius of the hydrogen atom.[28] Both classical and nonclassical hydrogen bonding have similar strength (3−12 kcal mol^{-1}) and display similar spectroscopic and electronic characteristics.[21,29,30]

There are reports of an increase in the reactivity of nonclassical hydrogen bonded M−H moieties,[31,32] leading in some cases to the activation of catalysts. For instance, Lau and co-workers recently provided compelling evidence that an intramolecular proton−hydride bond in $[(\eta^5\text{-}C_5H_4(CH_2)_nNMe_2H^+)RuH(dppm)]^+$ is a key feature in the catalytic hydrogenation of CO_2 to formic acid.[31] In addition, they also demonstrated that this intermediate is in equilibrium with a dihydrogen tautomer, $[(\eta^5\text{-}C_5H_4(CH_2)_nNMe_2)Ru(H_2)(dppm)]^+$, that reversibly liberates H_2. Noyori's group also showed that $[RuCl_2(\eta^6\text{-arene})]_2$ species react with chiral diamines to form complexes containing intramolecular proton−hydride bonds that efficiently catalyze the asymmetric hydrogenation of ketones to chiral alcohols.[32]

Most structurally characterized proton−hydride interactions typically show the proton and hydride bonded in an intramolecular fashion. However, Patel et al. provided an example of an intermolecular proton−hydride interaction in the solid state when they showed by a neutron diffraction study that the NH unit of indole when cocrystallized with $ReH_5(PPh_3)_3$ interacts with the hydride ligands.[33] Various other groups have also provided spectroscopic evidence for intermolecular nonclassical interactions in solution.[19,20,33−37]

We have found that anionic hydrides can form strong proton−hydride bonds.[38,39] The complexes [K(1-aza-18-crown-6)][$MH_3(CO)(P^iPr_3)_2$] (M = Os, Ru) were shown to be the first one-dimensional solids containing alternating intermolecular MH···HN hydride−proton and MCO···K bonds in the solid state.[39] In a recent communication we reported that the $[K(diaza\text{-}18\text{-}crown\text{-}6)]^+$ salts of $[OsH_5(P^iPr_3)_2]^-$ and $[IrH_4(P^iPr_3)_2]^-$ self-assemble to form linear chains held together by these proton−hydride bonds.[38] We now report the full details of the chemistry of the $[MH_5(P^iPr_3)_2]^-$ salts (M = Os, Ru). One of our primary objectives is to study the mechanism whereby these intermolecular proton−hydride interactions enhance the activity of the M−H bonds in the $[MH_5(P^iPr_3)_2]^-$ anions. This could possibly lead to practical applications since it is known that anionic hydride species are involved as intermediates and catalyst precursors in the hydrogenation of ketones, aldehydes, nitriles, esters, and olefins.[40−42]

Experimental Section

General Considerations. All preparations and manipulations were carried out under H_2, N_2, or Ar atmospheres with the use of standard Schlenk, vacuum line, and glovebox techniques in dry, oxygen-free solvents. Tetrahydrofuran (THF), diethyl ether (Et_2O), and hexanes were dried and distilled from sodium benzophenone ketyl. Deuterated solvents were degassed and dried over molecular sieves. Triisopropyl phosphine was supplied by Organometallics Inc., and KH, 18-crown-6, 1-aza-18-crown-6, and 1,10-diaza-18-crown-6 were supplied by Aldrich Chemical Co. $RuCl_3 \cdot xH_2O$ and $OsCl_3 \cdot xH_2O$ were obtained as a loan from Johnson Matthey Inc. $OsH_2Cl_2(PiPr_3)_2$ was prepared according to literature procedures.[43] The preparations of **1Os**, **3Os**, [K(aza-18-crown-6)][BPh_4], and [K(diaza-18-crown-6)][BPh_4] were outlined in our previous reports.[38,39] NMR spectra were recorded on a Varian Unity-500 (500 MHz for ^{1}H, 76.7 MHz for ^{2}H) or on a Varian Gemini 300 MHz spectrometer (300 MHz for ^{1}H and 121.5 for ^{31}P). All ^{31}P spectra were recorded with proton decoupling, and ^{31}P chemical shifts were measured relative to 85% H_3PO_4 as an external reference. ^{1}H chemical shifts were measured relative to partially deuterated solvent peaks but are reported relative to tetramethylsilane. ^{2}H chemical shifts were referenced to natural abundance deuterated solvent peaks. T_1 measurements were made at 500 MHz using the inversion recovery method. The temperature of the probe was calibrated using the temperature dependence of the chemical shifts of MeOH. NOESY and NOE spectra were also recorded at 500 MHz.

(15) Xu, W.; Lough, A. J.; Morris, R. H. *Inorg. Chem.* **1996**, *35*, 1549−1555.
(16) Morris, R. H. *Can. J. Chem.* **1997**, *74*, 1907-1915.
(17) Park, S. H.; Lough, A. J.; Morris, R. H. *Inorg. Chem.* **1996**, *35*, 3001−3006.
(18) Van Der Sluys, L. S.; Eckert, J.; Eisenstein, O.; Hall, J. H.; Huffman, J. C.; Jackson, S. A.; Koetzle, T. F.; Kubas, G. J.; Vergamini, P. J.; Caulton, K. G. *J. Am. Chem. Soc.* **1990**, *112*, 4831−4841.
(19) Peris, E.; Lee, J. C.; Rambo, J. R.; Eisenstein, O.; Crabtree, R. H. *J. Am. Chem. Soc.* **1995**, *117*, 3485−3491.
(20) Peris, E.; Wessel, J.; Patel, B. P.; Crabtree, R. H. *J. Chem. Soc., Chem. Commun.* **1995**, 2175−2176.
(21) Crabtree, R. H.; Siegbahn, P. E. M.; Eisenstein, O.; Rheingold, A. L. *Acc. Chem. Res.* **1996**, *29*, 348−354.
(22) Campbell, J. P.; Hwang, J. W.; Young, J. V. G.; von Dreele, R. B.; Cramer, C. J.; Gladfelter, W. L. *J. Am. Chem. Soc.* **1998**, *120*, 521−531.
(23) Epstein, L. M.; Shubina, E. S.; Bakhmutova, E. V.; Saitkulova, L. N.; Bakhmutov, V. I.; Chistyakov, A. L.; Stankevich, I. V. *Inorg. Chem.* **1998**, *37*, 3013−3017.
(24) Shubina, E. S.; Belkova, N. V.; Bakhmutova, E. V.; Saitkulova, L. N.; Ionidis, A. V.; Epstein, L. M. *Russ. Chem. Bull.* **1998**, *47*, 817−822.
(25) Richardson, T. B.; de Gala, S.; Crabtree, R. H. *J. Am. Chem. Soc.* **1995**, *117*, 12875−12876.
(26) Godfrey, P. D.; Grigsby, W. J.; Nichols, P. J.; Raston, C. L. *J. Am. Chem. Soc.* **1997**, *119*, 9283−9284.
(27) Morris, R. H. *Can. J. Chem.* **1996**, *74*, 1907−1915.
(28) Crabtree, R. H. *Science* **1998**, *282*, 2000−2001.
(29) Popelier, P. L. A. *J. Phys. Chem.* **1998**, *102*, 1873−1878.
(30) Liu, Q.; Hoffmann, R. *J. Am. Chem. Soc.* **1995**, *117*, 10108−10112.
(31) Chu, H. S.; Lau, C. P.; Wong, K. Y.; Wong, W. T. *Organometallics* **1998**, *17*, 2768−2777.
(32) Haack, K. J.; Hashiguchi, S.; Fujii, A.; Ikariya, T.; Noyori, R. *Angew. Chem., Int. Ed. Engl.* **1997**, *36*, 285−290.
(33) Patel, B. P.; Wessel, J.; Yao, W.; Lee, J. C.; Peris, E.; Koetzle, T. F.; Yap, G. P. A.; Fortin, J. B.; Ricci, J. S.; Sini, G.; Albinati, A.; Eisenstein, O.; Rheingold, A. L.; Crabtree, R. H. *New J. Chem.* **1997**, *21*, 413−421.
(34) Ayllon, J. A.; Gervaux, C.; Sabo-Etienne, S.; Chaudret, B. *Organometallics* **1997**, *16*, 2000−2002.
(35) Ayllon, J. A.; Sabo-Etienne, S.; Chaudret, B.; Ulrich, S.; Limbach, H. H. *Inorg. Chim. Acta* **1997**, *259*, 1−4.
(36) Shubina, E. S.; Belkova, N. V.; Krylov, A. N.; Vorontsov, E. V.; Epstein, L. M.; Gusev, D. G.; Niedermann, M.; Berke, H. *J. Am. Chem. Soc.* **1996**, *118*, 1105−1112.
(37) Bosque, R.; Maseras, F.; Eisenstein, O.; Patel, B. P.; Yao, W. B.; Crabtree, R. H. *Inorg. Chem.* **1997**, *36*, 5505−5511.
(38) Abdur-Rashid, K.; Gusev, D. G.; Landau, S. E.; Lough, A. J.; Morris, R. H. *J. Am. Chem. Soc.* **1998**, *120*, 11826−11827.
(39) Gusev, D. G.; Lough, A. J.; Morris, R. H. *J. Am. Chem. Soc.* **1998**, *120*, 13138−13147.
(40) Linn, D. E.; Halpern, J. *J. Am. Chem. Soc.* **1987**, *109*, 2969−2974.
(41) Grey, R. A.; Pez, G. P.; Wallo, A. *J. Chem. Soc., Chem. Commun.* **1980**, 783.
(42) Grey, R. A.; Pez, G. P.; Wallo, A. *J. Am. Chem. Soc.* **1981**, *103*, 7536.
(43) Aracama, M. A.; Estruelas, M. A.; Lahoz, F. J.; Lopez, J. A.; Meyer, U.; Oro, L. A.; Werner, H. *Inorg. Chem.* **1991**, *30*, 288.

Table 1. Summary of Crystal Data, Details of Intensity Collection, and Least Squares Refinement Parameters for 2Os, 1Ru, 2Ru, and 3Ru

	2Os	1Ru	2Ru	3Ru
M_r	890.23	802.08	801.10	728.01
cryst size, mm	0.20 × 0.15 × 0.15	0.32 × 0.29 × 0.18	0.30 × 0.25 × 0.24	0.35 × 0.30 × 0.23
cryst class	monoclinic	monoclinic	monoclinic	monoclinic
space group	$P2_1/c$	$P2_1/n$	$P2_1/c$	C_2/c
temp, K	150	150	100	150
a, Å	11.2075(2)	10.6070(3)	11.1699(10)	19.7329(4)
b, Å	19.0826(5)	34.103(1)	19.075(2)	11.7621(2)
c, Å	20.4912(5)	12.0417(3)	20.433(2)	17.2298(4)
β, deg	96.865(1)	93.078(2)	97.250(4)	102.679(1)
V, Å^3	4351(2)	4349.5(2)	4318.9(7)	3901.5(1)
Z	4	4	4	4
D_{calc} g cm^{-3}	1.359	1.225	1.232	1.239
μ(Mo Kα), mm^{-1}	3.137	0.568	0.587	0.622
F(000)	1856	1728	1728	1568
range θ collected, deg	4.09−26.36	4.15−26.38	4.09−26.34	4.10−26.37
no. of reflns	32 795	24 122	25 253	17 565
no. of ind reflns	8829	8781	8689	3976
R1[$I > 2\sigma(I)$][a]	0.0308	0.0377	0.0542	0.0286
wR2 (all data)[b]	0.0871	0.0877	0.1593	0.0790
goodness of fit	0.999	1.025	0.968	1.049
no. of params refined	414	441	425	231
max peak in final ΔF map, e Å^{-3}	0.786	0.419	1.095	0.680

[a] R1 = $\sum(F_o - F_c)/\sum(F_o)$. [b] wR2 = $[\sum[w(F_o^2 - F_c^2)^2]/\sum[w(F_o^2)^2]]^{1/2}$.

Infrared spectra were obtained on a Nicolet 550 Magna-IR spectrometer. Microanalyses were performed under an inert atmosphere by Guelph Chemical Laboratories Ltd., Ontario, Canada. All samples were submitted in ampules sealed under N_2. There is a systematic problem of substantially underestimated C% in the ruthenium complexes, although all H% and N% data are in very good agreement with the calculated values. We suspect that the low C% could result from the formation of metal carbides (upon thermal decomposition) and thus incomplete oxidation of carbon. The ^{1}H NMR measurements in all cases showed accurate integration.

X-ray Structure Analysis. Crystals of the complexes were prepared by slow diffusion of diethyl ether into THF solutions of the complexes under a nitrogen atmosphere. Crystals of **3Ru** were also prepared by layering a concentrated THF solution of **1Ru** with a saturated THF solution of [K(1,10-diaza-18-crown-6)][BPh_4]. Data were collected on a Nonius Kappa-CCD diffractometer using Mo Kα radiation (λ = 0.71073 Å). The CCD data were integrated and scaled using the DENZO-SMN software package, and the structures were solved and refined using SHELXTL V5.0. The crystallographic data for **2Os**, **1Ru**, **2Ru**, and **3Ru** are listed in Table 1. The hydrides in **1Os** and **1Ru** were located and refined with isotropic thermal parameters. The details of the crystal structures of **1Os** and **3Os** were reported elsewhere.[38]

Synthesis. [K(aza-18-crown-6)][$OsH_5(P^iPr_3)_2$], 2Os. THF (1 mL) was injected against a flow of H_2 into a flask containing a mixture of $OsH_2Cl_2(P^iPr_3)_2$ (95 mg, 0.16 mmol), KH (25 mg, 0.62 mmol), and 1-aza-18-crown-6 (45 mg, 0.16 mmol). After stirring for 4 h, the mixture was filtered and the solids washed with 2 × 0.5 mL of THF. Hexanes (5 mL) were added to the combined filtrate to precipitate a white solid. Yield = 98 mg (75%). ^{1}H NMR (THF-d_8): −12.39 (t, ^2J(HP) = 14.85 Hz, 5H, OsH), 1.10 (m, 36H, CH_3), 1.54 (m, 6H, CH), 2.10 (qi, 1H, NH), 2.74 (m, 4H, CH_2), 3.60 (m, 20H, CH_2). ^{31}P{^{1}H}: 63 (s). IR (Nujol): ν_{Os-H} 1835 (s), ν_{N-H} 3172 cm^{-1} (s, br). Anal. Calcd for $C_{30}H_{72}KO_5OsNP_2$: C, 44.04; H, 8.87; N, 1.71. Found: C, 44.26; H, 8.97; N, 1.63.

[K(18-crown-6)][$RuH_5(P^iPr_3)_2$], 1Ru. A mixture of $RuCl_3 \cdot xH_2O$ (500 mg, 2.1 mmol) and P^iPr_3 (840 mg, 5.24 mmol) in 5 mL of THF was stirred for 3 h at 60 °C and then evaporated to dryness. KH (841 mg, 21 mmol) and 18-crown-6 (550 mg, 2.08 mmol) were added to the black residue. THF (5 mL) was then injected into the flask against a flow of H_2, and the mixture stirred for 1 h under H_2, then for 2 h under N_2. The resulting mixture was filtered through Celite, and the solids were washed with 2 × 2.5 mL of THF. The white product was then precipitated by the addition of hexanes (10 mL), filtered, washed with 2 × 3 mL of THF/hexanes (1:2) and with 2 × 3 mL of hexanes, and dried in vacuo. Yield = 1.01 g (66%). ^{1}H NMR (THF-d_8): −9.25 (t, ^2J(HP) = 18.8 Hz, 5H, RuH), 1.12 (m, 36H, CH_3), 1.52 (m, 6H, CH), 3.65 (s, 24H, CH_2). ^{31}P{^{1}H}: 106.3 (s). IR (Nujol): ν_{Ru-H} 1769 (s), 1755 cm^{-1} (s). Anal. Calcd for $C_{30}H_{71}KO_6RuP_2$: C, 49.36; H, 9.80. Found: C, 44.57; H, 10.10.

[K(aza-18-crown-6)][$RuH_5(P^iPr_3)_2$], 2Ru. A mixture of $RuCl_3 \cdot xH_2O$ (250 mg, 1.05 mmol) and P^iPr_3 (420 mg, 2.62 mmol) in 5 mL of THF was stirred for 3 h at 60 °C and then evaporated to dryness. KH (420 mg, 10.5 mmol) and aza-18-crown-6 (275 mg, 2.08 mmol) were added to the black residue. THF (5 mL) was then injected into the flask against a flow of H_2, and the mixture stirred for 1 h under H_2. The resulting mixture was filtered, and the solids were washed with 2 × 1 mL of THF. The white product was then precipitated by the addition of hexanes (10 mL), filtered, washed with 2 × 2 mL of THF/hexanes (1:2) and with 2 × 2 mL of hexanes, and dried in vacuo. Yield = 398 mg (52%). ^{1}H NMR (THF-d_8): −9.24 (t, ^2J(HP) = 18.63 Hz, 5H, OsH), 1.13 (m, 36H, CH_3), 1.54 (m, 6H, CH), 2.38 (qi, 1H, NH), 2.74 (m, 4H, CH_2), 3.62 (m, 20H, CH_2). ^{31}P{^{1}H}: 105.1 (s). IR (Nujol): ν_{Ru-H} 1745 (s), ν_{N-H} 3168 cm^{-1} (s, br). Anal. Calcd for $C_{30}H_{72}KO_5RuNP_2$: C, 49.41; H, 9.96; N, 1.92. Found: C, 48.77; H, 10.09; N, 1.91.

[K(diaza-18-crown-6)][$RuH_5(P^iPr_3)_2$], 3Ru. A mixture of $RuCl_3 \cdot H_2O$ (100 mg, 0.42 mmol) and P^iPr_3 (168 mg, 1.05 mmol) in 2 mL of THF was stirred for 5 h at 60 °C and then evaporated to dryness. KH (168 mg, 4.2 mmol) and diaza-18-crown-6 (110 mg, 0.42 mmol) were added to the black residue. THF (2 mL) was then injected into the flask against a flow of H_2, and the mixture stirred for 2 h. The resulting mixture was filtered, and the solids were extracted with 3 × 10 mL of THF. The combined THF solutions were concentrated to 10 mL, and 15 mL of hexanes was then added, precipitating the white product. This was filtered, washed with hexanes, and dried in vacuo. Yield = 82 mg (30%). ^{1}H NMR (THF-d_8): −9.24 (t, ^2J(HP) = 18.5 Hz, 5H, RuH), 1.16 (m, 36H, CH_3), 1.54 (m, 6H, CH), 2.01 (qi, 2H, NH), 2.75 (m, 8H, CH_2), 3.58 (m, 16H, CH_2). ^{31}P{^{1}H}: 106.2 (s). IR (Nujol): ν_{Ru-H} 1750, ν_{N-H} 3173 cm^{-1} (s, br). Anal. Calcd for $C_{30}H_{73}KO_4RuN_2P_2$: C, 49.49; H, 10.11; N, 3.85. Found: C, 45.80; H, 9.90; N, 3.51.

Deuteration Studies. A sample of the complex, dissolved in the required solvent, was injected into a NMR tube under an argon or nitrogen atmosphere. The tube was then fitted with an adapter equipped with a Teflon stopcock and transferred to a vacuum line. The sample was cooled to liquid nitrogen temperature, degassed under vacuum, and then closed. When the contents of the tube reached room temperature, D_2 gas (1 atm) was back-filled into the tube, which was then closed, cooled to liquid nitrogen temperature, and sealed.

Results and Discussion

Synthesis and Structure of the Complexes. The osmium complexes $[K(Q)][OsH_5(P^iPr_3)_2]$ were prepared in 70−80% yield by reacting $OsH_2Cl_2(P^iPr_3)_2$ in the presence of THF and under 1 atm H_2 with excess potassium hydride and 1 equiv of the respective crown ether, Q (eq 1).

$$OsH_2Cl_2(P^iPr_3)_2 + 3KH + Q \xrightarrow{THF,\ H_2} [K(Q)][OsH_5(P^iPr_3)_2] + 2KCl \quad (1)$$

1Os, Q = 18-crown-6
2Os, Q = aza-18-crown-6
3Os, Q = diaza-18-crown-6

The ruthenium complexes $[K(Q)][RuH_5(P^iPr_3)_2]$ were prepared in 30−70% yields from the following one-pot reaction. A mixture of $RuCl_3/2.5P^iPr_3$ in THF was refluxed for 3 h and then evaporated to dryness. Excess potassium hydride, the respective crown ether, and THF were then added to the residue under 1 atm H_2 (eq 2).

$$RuCl_3.xH_2O \xrightarrow[(2)\ KH,\ Q,\ H_2,\ THF;\ -3KCl]{(1)\ P^iPr_3,\ THF} [K(Q)][RuH_5(P^iPr_3)_2] \quad (2)$$

1Ru, Q = 18-crown-6
2Ru, Q = aza-18-crown-6
3Ru, Q = diaza-18-crown-6

These complexes are air and water sensitive colorless salts. The $[K(18\text{-crown-6})]^+$ salts, **1Os** and **1Ru**, are very soluble in THF and only sparingly soluble in toluene and benzene, while the $[K(aza\text{-}18\text{-crown-6})]^+$ salts, **2Os** and **2Ru**, are very soluble in THF, toluene, and benzene. Solubility in the aromatic solvents could be due to the formation of 1:1 ion pairs, which would be enhanced in the case of **2Os** and **2Ru** due to the possibility of forming hydride−proton bonds between the MH and NH moieties. On the other hand the $[K(diaza\text{-}18\text{-crown-6})]^+$ salts, **3Os** and **3Ru**, are totally insoluble in benzene and toluene and only sparingly soluble in THF because of their propensity to form one-dimensional chain structures. Hence these salts were isolated by one of two methods: (1) repeatedly extracting their respective reaction mixtures with THF; (2) allowing the diffusion of $[K(diaza\text{-}18\text{-crown-6})]BPh_4$ into a solution of **1Os** or **1Ru** in THF (e.g., eq 3).

$$[K(diaza\text{-}18\text{-crown-6})]BPh_4 + [K(18\text{-crown-6})][RuH_5(P^iPr_3)_2] \xrightarrow{THF} \mathbf{3Ru}\downarrow + [K(18\text{-crown-6})]BPh_4 \quad (3)$$

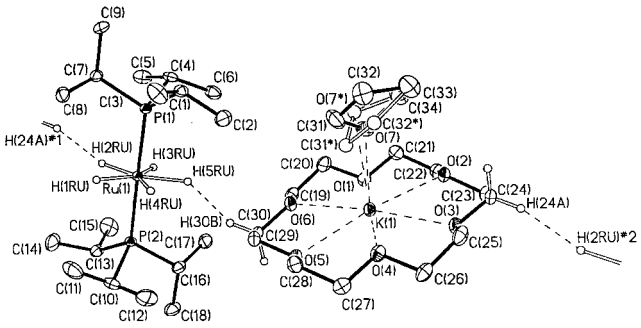

Figure 1. Molecular structure and atomic numbering of $[K(THF)(18\text{-crown-6})][RuH_5(P^iPr_3)_2]$. The cocrystallized THF molecule is disordered over two positions with site occupancies of 78.6 and 21.4%.

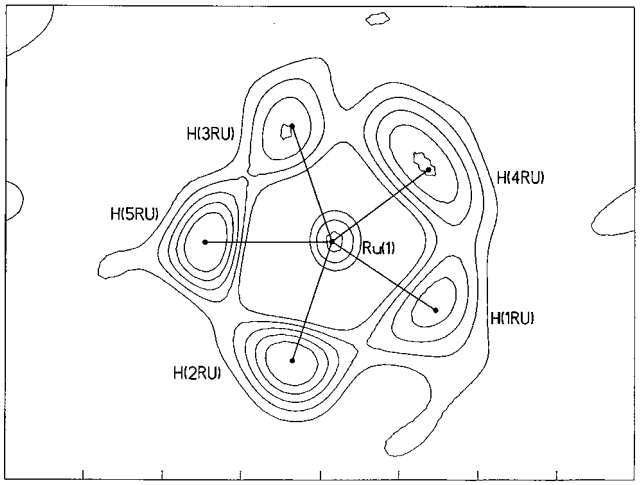

Figure 2. Difference electron density map around Ru, showing the positions of the hydride hydrogens in the anion of $[K(THF)(18\text{-crown-6})][RuH_5(P^iPr_3)_2]$. Contours are at the 1 e $Å^{-3}$.

Figure 1 shows the structure of **1Ru** as determined by X-ray diffraction. The previously reported structure of **1Os** is identical.[38] The salts crystallize with the cation $[K(THF)(18\text{-crown-6})]^+$ and anion $[MH_5(P^iPr_3)_2]^-$ in van der Waals contact. In each case the pentagon of hydride ligands is well-defined with all five H atoms located in a difference electron density map (Figure 2), and their positions refined isotropically. The potassium of the cation is slightly out of the crown ether plane due to the coordinated THF molecule, which in turn is disordered over two positions, as illustrated in Figure 1.

The M−H distances in the anions (Table 2) range from 1.48(4) to 1.63(5) Å (Os−H) and 1.54(3) to 1.60(3) Å (Ru−H). These values are relatively short compared with the average M−H distance of 1.65 Å, typical of second- and third-row transition metal hydrides, based on neutron diffraction studies.[44,45] This is probably due to the underestimation of bond lengths normally associated with X-ray diffraction since this method detects the electron density rather than nuclear positions. The bond angles between adjacent hydrides in the anions vary from 67(2)° to 77(2)° (osmium) and 70.5(15)° to 74.8(15)° (ruthenium). The bond angles between the phosphine and hydride ligands range from 86(2)° to

(44) Richardson, T. B.; Koetzle, T. F.; Crabtree, R. H. *Inorg. Chim. Acta* **1996**, *250*, 69−73.
(45) Drabnis, M. H.; Bau, R. *Inorg. Chim. Acta* **1997**, *259*, 27.

Table 2. Selected Bond Distances (Å) and Angles (deg) for [K(THF)(18-crown-6)][$MH_5(P^iPr_3)_2$]

	1Os	1Ru
M(1)−H(4M)	1.48(4)	1.54(3)
M(1)−H(3M)	1.55(4)	1.56(3)
M(1)−H(1M)	1.56(4)	1.59(3)
M(1)−H(2M)	1.57(4)	1.60(3)
M(1)−H(5M)	1.63(5)	1.60(3)
M(1)−P(2)	2.285(1)	2.2829(7)
M(1)−P(1)	2.290(1)	2.2872(7)
K(1)−O(6S)	2.703(4)	2.697(4)
K(1)−O(4)	2.741(3)	2.740(2)
K(1)−O(1)	2.770(3)	2.770(2)
K(1)−O(5)	2.769(3)	2.775(2)
K(1)−O(2)	2.817(3)	2.818(2)
K(1)−O(3)	2.820(3)	2.821(2)
K(1)−O(6)	2.823(3)	2.829(2)
K(1)−O(6S*)		3.16(3)
P(2)−M(1)−P(1)	176.88(3)	176.88(3)

92.1(13)° for the osmium complex and 86.6(11)° to 91.4(10)° for ruthenium.

The plane of the [K(THF)(18-crown-6)]$^+$ cation is approximately perpendicular to the P−M−P axis of the anion of **1Os** or **1Ru**. The closest distance between a hydride of the anion and a hydrogen on the [K(THF)(18-crown-6)]$^+$ cation in complex **1Os** is 2.4 Å. The only form of intermolecular interaction involves weak van der Waal's contacts, for example, between the potassium of the cation and the methyl hydrogens of a phosphine ligand of the anion. On the other hand, the structure of **1Ru** (Figure 1) also indicates the presence of weak intermolecular Ru−H···H−C interactions[44,46,47] of 2.2 Å between two of the hydrides of the anion (H2RU and H5RU) and methylene hydrogens (H24A#1 and H30B) of two adjacent [K(THF)(18-crown-6)]$^+$ cations.

The crystal structure of **3Ru** (Figure 3) is similar to the one previously reported for **3Os**, with the exception that the [K(1,10-diaza-18-crown-6)]$^+$ cation in the ruthenium complex has a rotational disorder of about 16° about the axis perpendicular to the ring. The occupancies of the two components are 0.87/0.13. The most obvious and significant variation of the structures of **3Os** and **3Ru** from those of **1Os** and **1Ru** is the steric disposition of the [K(1,10-diaza-18-crown-6)]$^+$ cation relative to that of the anion. The ensuing complementary inter-ion bonding produces a one-dimensional network in the solid-state structures of **3Os** and **3Ru**.

The individual ions in each structure are located on crystallographically imposed centers of inversion. The N−K−N axes of the [K(diaza-18-crown-6)]$^+$ cations are at an angle of 24° to the P−M−P axes of the [$MH_5(P^iPr_3)_2$]$^-$ anions and are oriented so that the NH groups are directed toward the hydride ligands of adjacent anions. The potassium in the plane of the crown forms axial K···HC interactions of 3.0 Å with the hydrogens of two adjacent phosphine methine groups. The refined N−H distance of 0.96(5) Å in **3Os** (Table 3) is comparable to the 1.00 Å of ammonium salts determined by neutron diffraction. The electron density map of the equatorial plane of the [$RuH_5(P^iPr_3)_2$]$^-$ anion in **3Ru** shows that the hydrides, though not individually located, are probably disordered over 10 sites in an

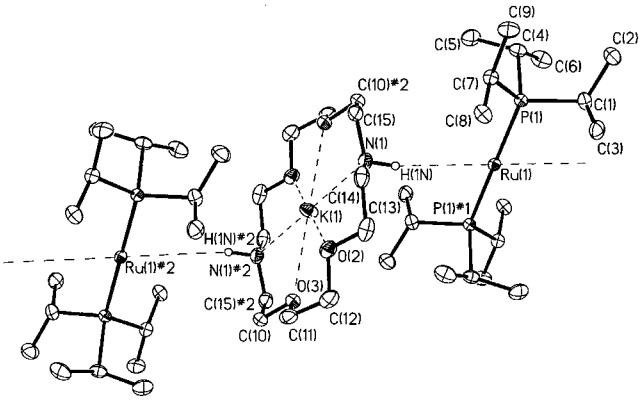

Figure 3. Molecular structure and atomic numbering of [K(1,10-diaza-18-crown-6)][$RuH_5(P^iPr_3)_2$], **3Ru**.

Table 3. Selected Bond Distances (Å) and Angles (deg) for [K(diaza-18-crown-6)][$MH_5(P^iPr_3)_2$]

	3Os	3Ru[a]
M(1)−P(1)#1	2.2931(8)	2.2941(5)
M(1)−P(1)	2.2931(8)	2.2941(5)
K(1)−O(2)#2	2.809(3)	2.821(2)
K(1)−O(2)	2.809(3)	2.821(2)
K(1)−O(3)	2.820(2)	2.828(2)
K(1)−O(3)#2	2.820(2)	2.828(2)
K(1)−N(1)#2	2.878(3)	2.880(2)
K(1)−N(1)	2.878(3)	2.880(2)
N(1)−H(1N)	0.96(5)	n.o.[b]
P(1)#1−M(1)−P(1)	180.0	180.0
N(1)#2−K(1)−N(1)	180.0	180.0

[a] Distances and angles in the disordered component are identical. [b] n.o. not observed

Scheme 1

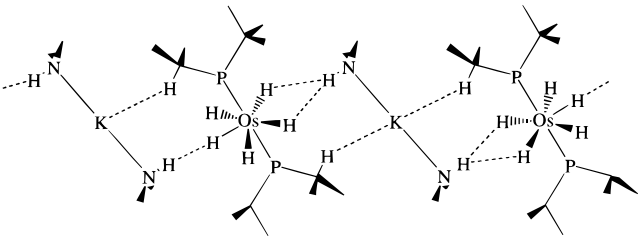

arrangement similar to the one reported in the neutron structure of $IrH_5(P^iPr_3)_2$, which also crystallizes with a center of inversion.[48]

The disorder of the hydride hydrogens in **3Os** and **3Ru** could arise from either static or dynamic processes. A static disorder would be the consequence of MH···HN bonding as illustrated in Scheme 1. This shows that on one side of the pentahydride anion an NH group of a cation is binding simultaneously to two of the hydrides in a bifurcated fashion with estimated H···H distances of about 2.1 Å. A similar bonding arrangement was observed in the neutron structure of $ReH_5(PPh_3)_3$·indole.[33] On the opposite side of the anion, a hydride is bonded end-on to the NH of the other adjacent cation with estimated H···H distances of 1.9 and 1.8 Å for **3Os** and **3Ru**, respectively. The observed disorder could arise if the bonding arrangement around the adjacent anion is either random or reversed in the same way as shown. A dynamic disorder would be the consequence of fluxionality and equivalence of the hydride ligands about

(46) Abramov, Y. A.; Brammer, L.; Klooster, W. T.; Bullock, R. M. *Inorg. Chem.* **1998**, *37*, 6317−6328.

(47) Braga, D.; de Leonardis, P.; Grepioni, F.; Tedesco, E.; Calhorda, M. J. *Inorg. Chem.* **1998**, *37*, 3337−348.

(48) Garlaschelli, L.; Khan, S. I.; Bau, R.; Longoni, G.; Koetzle, T. F. *J. Am. Chem. Soc.* **1985**, *107*, 7212−7213.

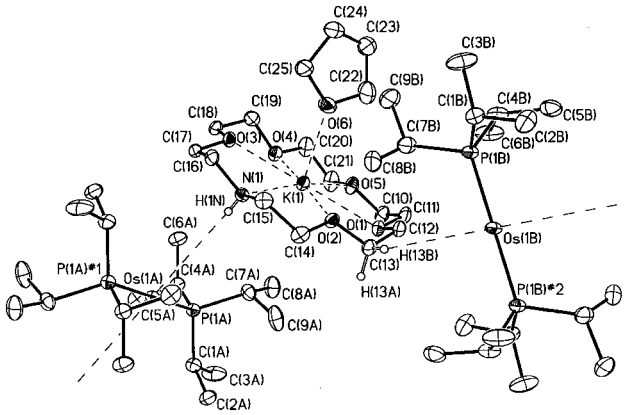

Figure 4. Molecular structure and atomic numbering of [K(THF)(aza-18-crown-6)][$OsH_5(P^iPr_3)_2$], **2Os**.

the plane of the anion in the solid state, resulting in a constant breaking and reforming of the NH···HM bonds.

Complexes **2Os** and **2Ru** crystallize as [K(THF)(1-aza-18-crown-6)][$MH_5(P^iPr_3)_2$]. The structure of **2Os** is shown in Figure 4 and is identical to that of **2Ru**. The osmium and ruthenium atoms are located at crystallographically imposed centers of inversion in their respective anions; hence the hydride hydrogens are not located. There are two halves of [$MH_5(P^iPr_3)_2$] anions associated with a [K(THF)(aza-18-crown-6)]$^+$ in the asymmetric unit with each half-anion located in a different chemical environment. The center of inversion relates the other half of the structural unit.

One anion is flanked by two [K(THF)(1-aza-18-crown-6)]$^+$ cations with their NH moieties directed to the pentagon of hydrides. The adjacent anion is in turn located between two [K(THF)(1-aza-18-crown-6)]$^+$ cations with one of the methylene protons of each (C13 in Figure 4) directed to the hydrides. The P−M−P axes of the anions of these two separate units are staggered relative to each other at an angle of about 72°, while the axes of identical units are parallel to each other. The net result is a zigzag pattern consisting of alternating NH···HMH···HN and CH···HMH···HC repeat units. This peculiar bonding arrangement is a possible consequence of the increased polarization and enhanced hydridicity of the anion resulting from the formation of a proton−hydride interaction with the NH unit of the [K(THF)(1-aza-18-crown-6)]$^+$ cation. Presumably, the subsequent formation of another proton−hydride bond (by the same anion) with the NH moiety of the adjacent cation is synergistically more favorable than an alternative arrangement involving the formation of discrete proton−hydride-bonded ion pairs. Additionally, the combined energy change associated with the formation of the NH···HM and CH···HM interactions is undoubtedly more favorable than that arising from the formation of discrete NH···HM bonded ion pairs. Intramolecular CH···HM bonding is a very common feature of polyhydride complexes,[17,44,49,50] particularly those containing aryl phosphines, and these bonds are expected to be about 60% as strong as their NH···HM counterparts, that is, approximately 2.5−3.5 kcal mol^{-1}.[44] The

Table 4. Selected Bond Distances (Å) and Angles (deg) for [K(THF)(aza-18-crown-6)][$MH_5(P^iPr_3)_2$]

	2Os	2Ru
M(1A)−P(1A)#1	2.2969(9)	2.293(1)
M(1A)−P(1A)	2.2969(9)	2.293(1)
M(1B)−P(1B)#2	2.290(1)	2.286(1)
M(1B)−P(1B)	2.290(1)	2.286(1)
K(1)−O(6)	2.690(3)	2.685(4)
K(1)−O(3)	2.742(3)	2.746(3)
K(1)−O(2)	2.762(3)	2.766(3)
K(1)−O(5)	2.804(3)	2.808(3)
K(1)−O(1)	2.831(3)	2.836(3)
K(1)−N(1)	2.840(4)	2.844(4)
K(1)−O(4)	2.857(3)	2.862(3)
N(1)−H(1N)	0.69(3)	0.81(3)
P(1A)#1−M(1A)−P(1A)	180.00(4)	180.00(5)
P(1B)#2−M(1B)−P(1B)	180.00(5)	180.00(7)

presence of the CH···HM interactions suggested by the solid-state structures of **2Os** and **2Ru** is particularly noteworthy since it was previously presumed that the proton-donor ability of a sp^3 C−H bond is not sufficient to facilitate intermolecular hydrogen bonding of this type.[44] However, there are a few recent reports of intermolecular proton−hydride bonds involving a carbon−hydrogen bond as the proton donor and at least one involving sp^3 C−H bonds.[46,47] The refined N−H distances in **2Os** and **2Ru** are 0.69(3) and 0.81(3) Å, respectively (Table 4), which are significantly shorter than the 1.00 Å value expected on the basis of neutron diffraction data in the literature. The OsH···HN and RuH···HN distances calculated using this latter value and assuming linear proton−hydride interactions are both 1.7 Å, which is substantially shorter than the 1.8−1.9 and 2.1 Å determined for linear and bifurcated OsH···HN and RuH···HN separations in **3Os** and **3Ru**. Similarly, the OsH···HC and RuH···HC distances are calculated to be 2.2 and 2.1 Å, respectively, if a value of 1.09 Å is used for the CH bond length. These MH···HC distances are shorter than the 2.4 Å estimated for just van der Waals contact but are similar to distances observed between phenyl ortho protons and hydrides in arylphosphine metal hydride complexes.[49] Even though the CH···HM interactions are weaker than the NH···HM bonds, they are evidently significant enough to contribute to the assembly of the one-dimensional chains adopted by **2Os** and **2Ru** in the solid state. The presence of these two types of interactions also explains the relatively higher solubilities of **2Os** and **2Ru** relative to **3Os** and **3Ru**, since in solution the weaker MH···HC bonds can be more readily disrupted to give discrete 1:1 ion pairs containing MH···HN interactions.

Infrared Spectra. The infrared spectrum of **1Os** in Nujol shows two Os−H bands of approximately equal intensity at 1858 and 1843 cm^{-1}. The spectrum of complex **1Ru** also displays a similar feature, with bands at 1769 and 1755 cm^{-1}. The higher energy of the Os−H vibrations is consistent with stronger bonding in the 5d metal.

The formation of hydrogen bonds is normally accompanied by characteristic changes in the infrared stretching frequencies of both the hydrogen bond donor and acceptor bands.[36] Likewise, the formation of MH···HX hydrogen bonds normally results in both the ν_{MH} and ν_{XH} bands broadening and shifting to lower wavenumbers. The infrared spectra (Nujol mull) of **2Os**, **3Os**, **2Ru**, and **3Ru** (Table 5) clearly indicate the presence

(49) Gini, G.; Eisenstein, O.; Yao, W.; Crabtree, R. H. *Inorg. Chim. Acta* **1998**, *280*, 26.
(50) Xu, W.; Lough, A. J.; Morris, R. H. *Can. J. Chem.* **1997**, *75*, 475−482.

Table 5. Summary of ^{1}H NMR (THF-d_8) and Infrared[a] Characteristics of the M−H and N−H Units of [K(Q)][BPh$_4$] and [K(Q)][MH$_5$(P^{i}Pr$_3$)$_2$] Salts

complex	unit	ν(M−H)/cm^{-1}	ν(N−H)/cm^{-1}	δ(N−H)/ppm
[K(1-aza-18-crown-6)][BPh$_4$]	N−H		3296 (3283)	0.92
[K(1,10-diaza-18-crown-6)][BPh$_4$]	N−H		3297 (3278, 3282)	1.00
[K(18-crown-6)][OsH$_5$(P^{i}Pr$_3$)$_2$], **1Os**	Os−H	1836 (1858, 1843)		
[K(1-aza-18-crown-6)][OsH$_5$(P^{i}Pr$_3$)$_2$], **2Os**	Os−H···HN	1833 (1835)	3168 3297[b] (3172)	2.10
[K(1,10-diaza-18-crown-6)][OsH$_5$(P^{i}Pr$_3$)$_2$], **3Os**	Os−H···HN	1835 (1839)	3184 3297[b] (3184)	1.89[c]
[K(18-crown-6)][RuH$_5$(P^{i}Pr$_3$)$_2$], **1Ru**	Ru−H	1747 (1769, 1755)		
[K(1-aza-18-crown-6)][RuH$_5$(P^{i}Pr$_3$)$_2$], **2Ru**	Ru−H···HN	1745 (1745)	3154 3296[b] (3168)	2.38
[K(1,10-diaza-18-crown-6)][RuH$_5$(P^{i}Pr$_3$)$_2$], **3Ru**	Ru−H···HN	1747 (1750)	3160 3296[b] (3173)	2.01[c]

[a] THF (values from Nujol mulls in parentheses). [b] Nonbonded NH. [c] Average for hydride-bonded and nonbonded NH.

of MH···HN bonding. The Os−H bands of **2Os** and **3Os** are broadened and more intense than the free Os−H vibration in **1Os** and shifted to 1835 and 1839 cm^{-1}, respectively. Likewise, the ν_{Ru-H} stretching modes in **2Ru** and **3Ru** are also broadened and more intense relative to the ν_{Ru-H} bands in **1Ru** and shifted from about 1760 in **1Ru** to 1745 and 1750 cm^{-1}, respectively. The change is even more significant for the ν_{N-H} band. The NH bands are broadened, more intense, and lowered by 96 cm^{-1} in **3Os** and 107 cm^{-1} in **3Ru** relative to the average ν_{N-H} of 3280 cm^{-1} of [K(1,10-diaza-18-crown-6)][BPh$_4$]. For **2Os** and **2Ru** the corresponding ν_{N-H} shifts to lower frequencies are by 111 and 115 cm^{-1}, respectively, relative to [K(1-aza-18-crown-6)][BPh$_4$] (3283 cm^{-1}). The greater shifts observed for the NH stretching wavenumber for **2Ru** and **3Ru** relative to **2Os** and **3Os** are caused by the greater basicity and hydridicity of the ruthenium complexes, since it is known that the pK_a of OsH$_6$(P^{i}Pr$_3$)$_2$, the conjugate acid of [OsH$_5$(P^{i}Pr$_3$)$_2$]$^-$, is 4 units less than that of RuH$_6$(P^{i}Pr$_3$)$_2$, the conjugate acid of the ruthenium anion.[51] The relative change in the ν_{Os-H}, ν_{Ru-H}, and ν_{N-H} modes implies that the MH···HN interactions in **2Os** and **2Ru** are stronger than those of **3Os** and **3Ru**, respectively. This is consistent with the proton−hydride distances in **2Os** and **2Ru** being 0.2 and 0.1 Å shorter than in **3Os** and **3Ru**, respectively. The change in the ν_{NH} vibrations for the complexes reflects the strengths of the proton−hydride bonds. Various relationships have been proposed to quantify $\Delta\nu_{XH}$ in terms of the bonding enthalpy.[36] The most widely used are a series of equations proposed by Iogansen, initially for organic molecules but which have been proposed to be equally applicable to organometallic systems and for nonclassical MH···HX and BH···HX bonds.[36] In one form, the enthalpy change is given by $\Delta H° = -0.3(\Delta\nu_{XH})^{1/2}$, where $\Delta\nu_{XH}$ represents the change in the XH stretching band of the hydrogen-bonded species relative to the free XH. Using this relationship, values of about −3 kcal mol^{-1} are obtained for the proton−hydride bonding enthalpies for complexes **2** and **3**.

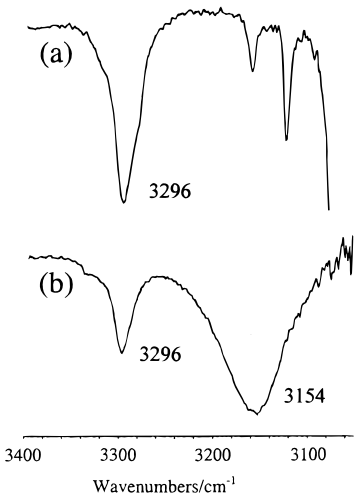

Figure 5. Solution (THF) infrared spectra in the ν_{NH} region of (a) [K(aza-18-crown-6)][BPh$_4$] and (b) [K(aza-18-crown-6)][RuH$_5$(P^{i}Pr$_3$)$_2$].

The solution (THF) infrared spectra of the complexes (Table 5) clearly indicate the persistence of proton−hydride interactions in solution. The spectra of **2Os** and **2Ru** show broad and intense NH bands at 3168 and 3154 cm^{-1}, respectively, down from 3296 cm^{-1} in a solution of [K(1-aza-18-crown-6)][BPh$_4$]. This is illustrated in Figure 5. The spectra of **2Os** and **2Ru** also show the presence of a free NH band at 3297 cm^{-1}. The Os−H and Ru−H bands are also broadened and shifted to 1833 and 1745 cm^{-1}, respectively. The free NH band indicates that there is equilibrium between the proton−hydride-bonded and free NH species in solutions of **2Os** and **2Ru**, as illustrated in Scheme 2.

The solution IR spectrum of **3Os** shows two bands of approximately equal intensities at 3297 and 3184 cm^{-1}, with the second band being much broader than the first. The corresponding ν_{NH} bands in the solution spectrum of **3Ru** are at 3296 and 3160 cm^{-1}. This indicates that **3Os** and **3Ru** exist as discrete ion pairs in solution in

(51) (a) Abdur-Rashid, K.; Fong, T. P.; Greaves, B.; Gusev, D. G.; Landau, S. E.; Lough, A. J.; Morris, R. H. Manuscript submitted. (b) Abdur-Rashid, K.; Gusev, D.; Lough, A. J.; Morris, R. H. Manuscript submitted.

Scheme 2

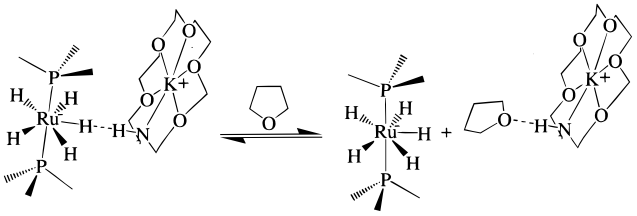

which one of the NH groups of the [K(diaza-18-crown-6)]$^+$ cation (at lower wavenumber) is proton−hydride bonded to a hydride while the other is free. The single chemical shift for the NH that is present in the ^{1}H NMR spectrum of **3Os** and **3Ru** is indicative of a very fast dynamic equilibrium involving the bonded and nonbonded NH groups. The solution $\Delta\nu_{NH}$ values of 128, 113, 142, and 136 cm^{-1}, for **2Os**, **3Os, 2Ru**, and **3Ru**, respectively, imply that the ion-pair-assisted proton−hydride interactions in solution are significantly greater than in the solid state. A bimolecular associative process in solution would typically involve entropy changes of −5 to −20 cal mol^{-1} K^{-1}. This would result in an energy barrier of 1.5 to 6 kcal mol^{-1} against bond formation at 298 K. It is also known that solvent interactions can prevent the formation of both intra- and intermolecular proton−hydride bonds. In particular, it has been demonstrated that proton acceptor solvents such as tetrahydrofuran can readily disrupt MH···HN interactions in solution.[11,15,17,27] Thus, the favorable electrostatic contribution to the formation of inter-ion pair proton−hydride bonds in THF solutions of **2Os**, **3Os**, **2Ru**, and **3Ru** is significant enough to overcome the opposing contributions from entropy and solute−solvent interactions.

NMR Studies. The NMR spectra of the anions are characteristic of a pentagonal bipyramidal structure. The hydride region of **1Os** shows a triplet at −12.4 ppm (J_{HP} = 14.9 Hz), while the ^{31}P{^{1}H} NMR shows a sharp singlet at 64.0 ppm. The analogous ruthenium complex shows a triplet at −9.25 ppm (J_{HP} = 18.8 Hz) and a singlet at 106.3 ppm in the ^{1}H and ^{31}P{^{1}H} NMR spectra, respectively. The ^{31}P NMR data are also consistent with the general observation that δP_{Ru} is approximately equal to δP_{Os} + 40 for isostructural osmium and ruthenium complexes.

The existence of proton−hydride bonding in solution is normally accompanied with perturbation of both the proton donor and hydride resonances in the ^{1}H NMR spectrum. Typically, it has been observed that for species with nonclassical hydrogen bonds the proton and hydride resonances display downfield and upfield shifts, respectively.[36] The ^{1}H NMR N−H resonances of **2Os**, **3Os**, **2Ru**, and **3Ru** (Table 5) provide evidence for the persistence of short intermolecular proton−hydride contacts in solution. The ^{1}H NMR spectra of [K(diaza-18-crown-6)][BPh$_4$] and [K(aza-18-crown-6)][BPh$_4$] in THF-d_8 show the free NH signal at 1.00 and 0.92 ppm, respectively (Table 5). The NH signal is shifted downfield to 1.89 ppm in **3Os** and 2.01 ppm in **3Ru**, while for **2Os** and **2Ru** the NH resonances are shifted downfield to 2.10 and 2.38 ppm, respectively. The weakening of the NH bond, as evidenced by the deshielding of the NH resonance, is indicative of proton−hydride contacts in the solutions of the complexes. The greater changes in the NH chemical shifts for the ruthenium complexes compared to the osmium analogues indicate that the proton−hydride interactions in the former are stronger. Even though the solution infrared data clearly demonstrate that the MH···HN interactions in the [K(aza-18-crown-6)]$^+$ complexes are enhanced relative to the respective [K(diaza-18-crown-6)]$^+$ salts in solution, it is more difficult to make a similar deduction from the NMR data, since the chemical shifts for these salts represent the average for both the free and proton−hydride bonded NH moieties.

Table 6. Summary of ^{1}H NMR T_1 Values (THF-d_8, 500 MHz) for the NH and MH$_5$ Moieties in [K(Q)][MH$_5$(P^{i}Pr$_3$)$_2$]; Q = 1-Aza-18-crown-6 and 1,10-Diaza-18-crown-6

	T_1/ms					
	2Ru		3Ru		3Os	
temp/K	RuH$_5$	NH	RuH$_5$	NH	OsH$_5$	NH
294			1244	1200	1316	1780
273			1041	1290	1002	658
252	920	513	909	1138	854	500
231	864	427		828	781	435
210	776	388	829	595	767	426
189	780	388	850	497	761	548
168	830	564				

Variable-temperature NMR experiments show changes in the hydride and NH chemical shifts with temperature. On lowering the temperature of a THF-d_8 solution of **3Os**, there is broadening of the NH resonance at 1.89 ppm (293 K) and further shifting downfield to 2.14 ppm (193 K), while the hydride resonance at −12.38 ppm (293 K) is shifted upfield to −12.45 ppm (193 K). The changes for **2Ru** are even more significant. The NH quintet at 2.38 ppm (293 K) is broadened and shifted downfield to 2.63 ppm at 183 K, while the hydride resonance correspondingly shifted upfield from −9.24 ppm to −9.33 ppm.

The NH proton of **2Ru** has a minimum T_1 of 388 ms at 213 K and 500 MHz (Table 6). The calculated NH···HRu distance using this value and accounting for the dipolar contribution of ^{14}N is 1.9 Å. The minimum T_1 value for complex **3Os** is 426 ms, from which a NH···HOs distance of 2.0 Å is determined. Even though this value for the osmium complex is comparable to the 1.9 Å obtained from analysis of the X-ray structural data, the NH···HOs distance is likely to be shorter and presumably closer to the 1.9 Å obtained for **2Ru**, since the minimum T_1 value for **3Os** represents an average of the free and proton−hydride bonded NH.

Further evidence for direct dipolar interactions between the hydrides of the [MH$_5$(P^{i}Pr$_3$)$_2$]$^-$ anions and the NH moieties of the [K(crown ether)]$^+$ cations in solution is provided by NOE difference (Figure 6) and NOESY experiments. Irradiation of the hydride signals in **2Os**, **3Os**, **2Ru**, and **3Ru** results in enhancements of the NH chemical shifts (10−12%) of the crown ether and the methyl and methine resonances of the phosphine ligands. Likewise, irradiation of the NH resonance results in enhancement of the hydride signal (4−6%) and the CH$_2$ signals of the crown ethers. The enhancement of the phosphine resonances on irradiation of the hydride signal is expected on account of the proximity of these hydrogens to the hydrides. Similarly, irradiation of the NH would concomitantly lead to an enhancement in the ^{1}H NMR signal of the β-CH$_2$ hydrogens.

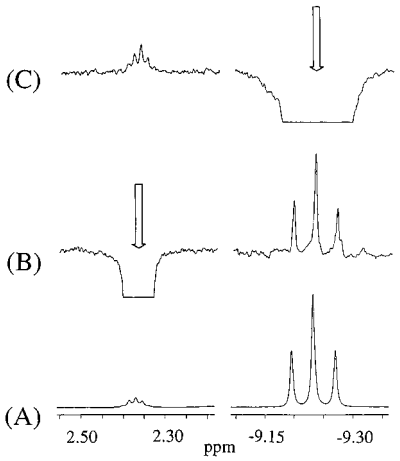

Figure 6. ^{1}H NMR (A) and ^{1}H NOE difference (B, C) spectra of the NH (2.38 ppm) and hydride (−9.24 ppm) regions of [K(aza-18-crown-6)][$RuH_5(P^iPr_3)_2$], **2Ru**, in THF-d_8. Arrows indicate the irradiated positions.

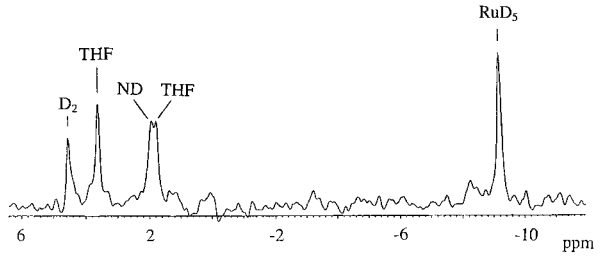

Figure 7. ^{2}H NMR spectrum of [K(1,10-diaza-18-crown-6)][$RuH_5(P^iPr_3)_2$] in THF under 1 atm D_2 gas.

Scheme 3

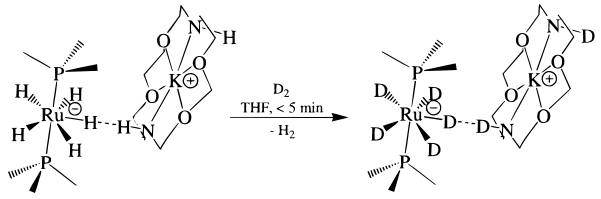

Deuteration Studies. The complexes containing proton−hydride bonds undergo H/D exchange upon exposure to D_2 gas at 1 atm and room temperature in THF, with both the NH and hydride resonances decreasing in intensity. In the case of **3Os** only 15% of the NH and hydride intensities could be detected after 10 days, while for **3Ru**, 100% of the intensity of the NH and 90% of the hydride resonance disappeared within 5 min under 1 atm D_2 gas at room temperature. The ^{2}H NMR spectrum of a solution of [K(diaza-18-crown-6)][$RuH_5(P^iPr_3)_2$] in THF under 1 atm of D_2 gas at room temperature (Figure 7) confirms the incorporation of deuterium into the NH of the [K(diaza-18-crown-6)]$^+$ cation and the hydrides of the [$RuH_5(P^iPr_3)_2$]$^-$ anion (Scheme 3).

The deuteration results provide further evidence of close proton−hydride contacts between the hydrides and NH in solutions of these complexes. In control experiments, where **1Os** and **1Ru** are exposed to D_2 gas at 1 atm and room temperature, no H/D exchange is detected for **1Os** and only a 13% decrease in the hydride resonance of **1Ru** after 10 days and 30% after 4 months. The mechanism for deuteration of the NH and hydrides of the salts containing proton−hydride bonds could presumably involve the intermediacy of the conjugate acids of the osmium and ruthenium pentahydrides. $OsH_6(P^iPr_3)_2$[52] is known to be a classical hydride, whereas the analogous ruthenium species is nonclassical and is more appropriately formulated as $RuH_2(H_2)_2(P^iPr_3)_2$ (**4**), implicating the presence of two coordinated dihydrogen ligands.[51,53] The disparity in the rates of H/D exchange for the osmium and ruthenium salts is consistent with the structural, electronic, and pK_a differences between their conjugate analogues. In separate experiments we demonstrate that **4** also readily undergoes H/D exchange with D_2 gas both in the solid state and in solution. The ^{2}H NMR spectrum of **4** in THF under 1 atm of D_2 shows that in addition to deuteration of the hydride ligands there is also extensive H/D exchange with the methyl hydrogens of the phosphine ligands.[51b] On the other hand, there is no H/D exchange with the phosphine methyl protons in **3Ru**. This implies that the mechanism of deuteration of **3Ru** may not involve **4** as an intermediate. This was supported by an experiment that involved preparing an equimolar mixture of **4** and [K(diaza-18-crown-6)][BPh_4] in THF-d_8 under D_2 gas. The ^{1}H NMR spectrum of the mixture shows the incorporation of deuterium only in the hydrides in **4**. On the other hand, a similar experiment with an equimolar mixture of **2Ru** and [K(diaza-18-crown-6)][BPh_4] shows the incorporation of deuterium in the hydrides of the pentahydride anion and the NH moieties of the two cations. Thus, it is evident that the increased rate of deuteration of the salts containing proton−hydride bonds relative to **1Os** and **1Ru** implies very efficient activation of the M−H bonds as a result of the nonclassical hydrogen bonding. Even though the mechanism for this enhanced activation is not immediately obvious, it is known that some of the most active homogeneous hydrogenation catalysts contain functionalities that could foster the formation of nonclassical hydrogen bonding.[32]

Conclusion

Inter-ion proton−hydride NH···HM interactions exist in complexes **2Os**, **3Os**, **2Ru**, and **3Ru**. In addition, inter-ion CH···HM interactions are present in the solid-state structures of **2Os**, **1Ru**, and **2Ru**. The presence of the NH···HM bonds causes lower wavenumber shifts in both the ν_{NH} and ν_{MH} bands in the infrared spectra of the complexes and increases the chemical shift of the NH in the ^{1}H NMR spectra. The infrared spectra of the complexes in THF solutions clearly indicate the important role of ion-pair assistance in the enhancement and stabilization of these nonclassical hydrogen bonds even in the presence of other hydrogen bond acceptor species (THF). The role of these interactions in influencing the solid-state structures of **2Os**, **3Os**, **2Ru**, and **3Ru** is illustrated by the one-dimensional chain structures adapted by these complexes. On this basis it is possible that suitably constructed species could also be used for the generation of two- and three-dimensional structures containing these nonclassical hydrogen bonds. Such

(52) Howard, J. A. K.; Johnson, O.; Koetzle, T. F.; Spencer, J. L. *Inorg. Chem.* **1987**, *26*, 2930−2933.
(53) Sabo-Etienne, S.; Chaudret, B. *Coord. Chem. Rev.* **1998**, *180*, 381−407.

materials could possibly be useful for catalysis, hydrogen storage, or hydrogen sensing. The enhanced activity of the salts containing proton−hydride bonds, as evidenced by their rates of H/D exchange with D_2 gas, also establishes the role of these interactions in promoting activation of the metal−hydride bonds, which could play a significant role in homogeneous catalytic hydrogenation processes. Finally, the infrared, NMR, H/D exchange, and X-ray data indicate that the strength of these ion-pair-assisted proton−hydride bonds is directly related to the basicity of the polyhydride anions.

Acknowledgment. This work was supported by a grant to R.H.M. from NSERC of Canada and a loan of osmium and ruthenium salts from Johnson Matthey Ltd. Dr. Howard Hunter and Dr. Timothy Burrow are gratefully acknowledge for assistance with the high-field NMR studies.

Supporting Information Available: X-ray crystallographic tables for complexes **2Os**, **1Ru**, **2Ru**, and **3Ru**. This material is available free of charge via the Internet at http://pubs.acs.org.

OM9908837